AD-A176 544 INTERPRETATION OF EXPERIMENTAL RESULTS IN THE SINGLE FILAMENT PULL-OUT TEST(U) MIDWEST RESEARCH INST KANSAS CITY MO L S PENN ET AL. 28 JAN 87 TR-2 1/1

UNCLASSIFIED N00014-84-C-0522 F/G 11/4 NL

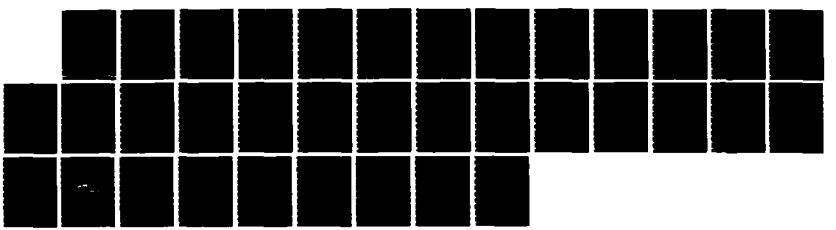

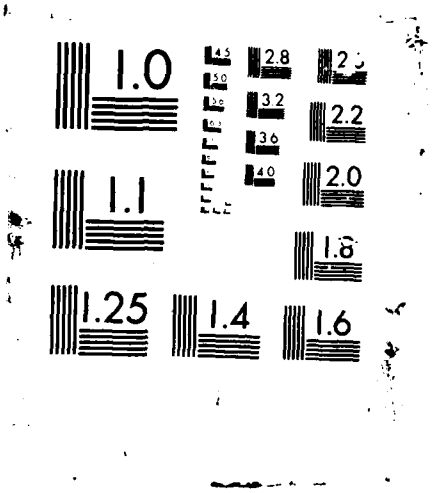
1.0
1.1
1.25
1.4
1.6
1.8
2.0
2.2
2.8
3.2
3.6
4.0

AD-A176 544

REPORT DOCUMENTATION PAGE

1a REPORT SECURITY CLASSIFICATION: Unclassified	1b RESTRICTIVE MARKINGS: None
2a SECURITY CLASSIFICATION AUTHORITY	3 DISTRIBUTION/AVAILABILITY OF REPORT: This document has been approved for public release and sale; its distribution is unlimited
2b DECLASSIFICATION/DOWNGRADING SCHEDULE	
4 PERFORMING ORGANIZATION REPORT NUMBER(S): Technical Report No. 2	5 MONITORING ORGANIZATION REPORT NUMBER(S)
6a NAME OF PERFORMING ORGANIZATION: Midwest Research Institute; 6b OFFICE SYMBOL (If applicable)	7a NAME OF MONITORING ORGANIZATION: Office of Naval Research
6c ADDRESS (City, State, and ZIP Code): 425 Volker Boulevard, Kansas City, Missouri 64110	7b ADDRESS (City, State, and ZIP Code): 800 North Quincy Street, Arlington, Virginia 22217
8a NAME OF FUNDING/SPONSORING ORGANIZATION: Office of Naval Research; 8b OFFICE SYMBOL (If applicable): ONR	9 PROCUREMENT INSTRUMENT IDENTIFICATION NUMBER: N0014-84-C-0522
8c ADDRESS (City, State, and ZIP Code): 800 North Quincy Street, Arlington, Virginia 22217	10 SOURCE OF FUNDING NUMBERS: PROGRAM ELEMENT NO; PROJECT NO; TASK NO; WORK UNIT ACCESSION NO

11 TITLE (Include Security Classification): Interpretation of Experimental Results in the Single Filament Pull-Out Test (Unclassified).

12 PERSONAL AUTHOR(S): Penn, L.S., and Lee. S.M.

13a TYPE OF REPORT	13b TIME COVERED FROM ____ TO ____	14 DATE OF REPORT (Year, Month, Day)	15 PAGE COUNT
Publication		1987, Jan. 28	

16 SUPPLEMENTARY NOTATION: Submitted to Composite Technology and Research

17 COSATI CODES: FIELD / GROUP / SUB-GROUP	18 SUBJECT TERMS (Continue on reverse if necessary and identify by block number): Fiber-matrix interface, single filament pull-out test, composite, geometry dependence

19 ABSTRACT (Continue on reverse if necessary and identify by block number)

The experimental results of the single filament pull-out test which is used to directly examine fiber-matrix interface bond strength are interpreted using a fracture mechanics approach. The nonlinear relation between the pull-out (debond) load and the fiber-matrix interfacial area is explained by considering the separate contributions of the matrix and the fiber to the interface failure process. In addition, the large experimental scatter is demonstrated to be inherent in the small test specimen size and to be caused by fiber surface energy heterogeneity.

20 DISTRIBUTION/AVAILABILITY OF ABSTRACT: X UNCLASSIFIED/UNLIMITED ☐ SAME AS RPT ☐ DTIC USERS	21 ABSTRACT SECURITY CLASSIFICATION: Unclassified	
22a NAME OF RESPONSIBLE INDIVIDUAL: Dr. Harold Guard	22b TELEPHONE (Include Area Code): 202-696-4410	22c OFFICE SYMBOL

DD FORM 1473, 84 MAR — 83 APR edition may be used until exhausted. All other editions are obsolete. SECURITY CLASSIFICATION OF THIS PAGE

TECHNICAL REPORT DISTRIBUTION LIST, GEN

	No. Copies
Office of Naval Research Attn: Code 1113 800 N. Quincy Street Arlington, Virginia 22217-5000	2
Dr. Bernard Douda Naval Weapons Support Center Code 50C Crane, Indiana 47522-5050	1
Naval Civil Engineering Laboratory Attn: Dr. R. W. Drisko, Code L52 Port Hueneme, California 93401	1
Defense Technical Information Center Building 5, Cameron Station Alexandria, Virginia 22314	12 high quality
DTNSRDC Attn: Dr. H. Singerman Applied Chemistry Division Annapolis, Maryland 21401	1
Dr. William Tolles Superintendent Chemistry Division, Code 6100 Naval Research Laboratory Washington, D.C. 20375-5000	1
Dr. David Young Code 334 NORDA NSTL, Mississippi 39529	1
Naval Weapons Center Attn: Dr. Ron Atkins Chemistry Division China Lake, California 93555	1
Scientific Advisor Commandant of the Marine Corps Code RD-1 Washington, D.C. 20380	1
U.S. Army Research Office Attn: CRD-AA-IP P.O. Box 12211 Research Triangle Park, NC 27709	1
Mr. John Boyle Materials Branch Naval Ship Engineering Center Philadelphia, Pennsylvania 19112	1
Naval Ocean Systems Center Attn: Dr. S. Yamamoto Marine Sciences Division San Diego, California 91232	1

ABSTRACT

The experimental results of the single filament pull-out test which is used to directly examine fiber-matrix interface bond strength are interpreted using a fracture mechanics approach. The nonlinear relation between the pull-out (debond) load and the fiber-matrix interfacial area is explained by considering the separate contributions of the matrix and the fiber to the interface failure process. In addition, the large experimental scatter is demonstrated to be inherent in the small test specimen size and to be caused by fiber surface energy heterogeneity.

KEYWORDS

Fiber-matrix interface, single-filament pull-out test, inherent scatter, fiber-dominated interface failure, matrix-dominated interface failure, geometry dependence.

A1

INTERPRETATION OF EXPERIMENTAL RESULTS IN THE SINGLE FILAMENT TEST

BY

L.S. PENN
CHEMICAL ENGINEERING DEPARTMENT
POLYTECHNIC UNIVERSITY
Brooklyn, New York 11201
AND

S.M. LEE
COMPOSITE MATERIALS DEPARTMENT
CIBA GEIGY CORPORATION
Fountain Valley, California 92728

I. INTRODUCTION

Various forms of the single filament pull-out test have been adopted to directly measure the adhesive performance of the fiber-matrix interface in fiber composite materials (1-5). Such a test gives more information about the interface itself than does a test on a realistic multifilament composite specimen. Independent characterization of the mechanical properties of the interface at the microscopic level promotes a clearer understanding of its effect on the bulk properties of the composite.

The single filament test has two major drawbacks that detract from its usefulness. The first is a geometry dependence of the results that has not been adequately rationalized up to now. The second is large scatter in the data, even when the number of specimens is large. These conditions make it harder to draw unambiguous conclusions from the single filament test results. This paper reports our detailed examination of both of these drawbacks. We have found that the geometry dependence can be understood in terms of fracture

mechanics and that the data scatter can be explained by inherent interfacial energy variation.

II. BACKGROUND

The basic geometry of the single filament test is that of a vertical filament which has a portion of its length embedded in a small volume of cured matrix. Some acceptable test geometries are shown in Figure 1.

Each pull-out experiment yields a force versus displacement trace as shown in Figure 2. The interfacial adhesive bond strength is usually defined to be τ, which is the maximum load P_m divided by the total interfacial area A. In this case $A=2\pi r\ell$, where r is fiber radius and ℓ is embedded length of the fiber before testing. The use of τ as defined here implies a simultaneous debonding of the whole bonded area, A, which can result only from a uniform stress distribution. However, detailed analyses have shown the stress distribution at the interface to be highly nonuniform with a stress concentration existing where the fiber enters the matrix (6). Such a stress concentration will be likely to promote progressive failure from the top of the interface to the bottom. This situation would not be expected to produce a linear relation between the maximum (pull-out) load and the initial embedded length. Models using either the maximum stress criterion (6,7,8) or the energy criterion (9, 10) have been used to predict and also to explain the observed P_m versus ℓ relation. It is particularly important to understand this relation because P_m and ℓ are the quantities obtained directly from the single filament pull-out test and they are used to compute other quantities. In our treatment we use the energy criterion to qualitatively predict P_m as a function of ℓ. Our interpretation differs from those of

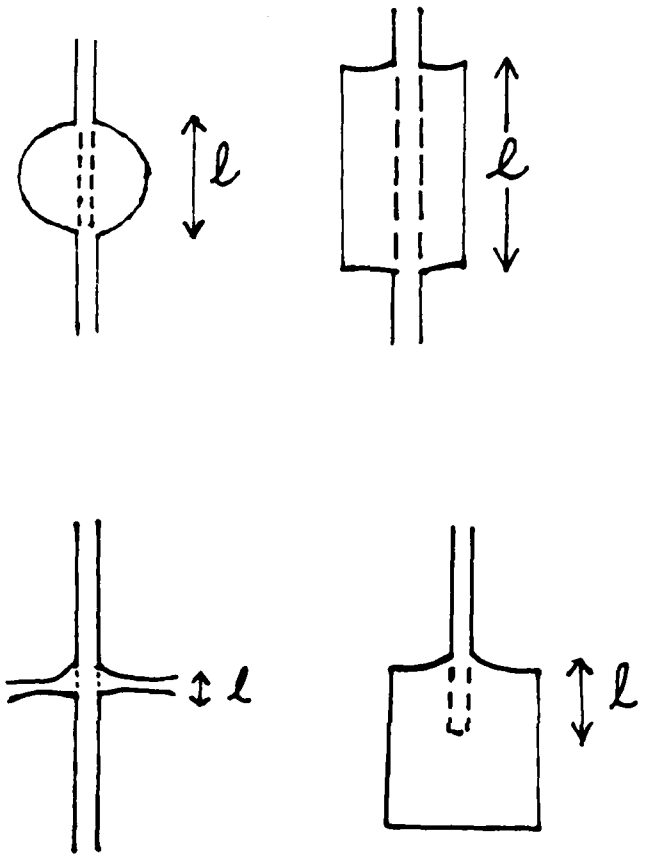
l
l
l
l

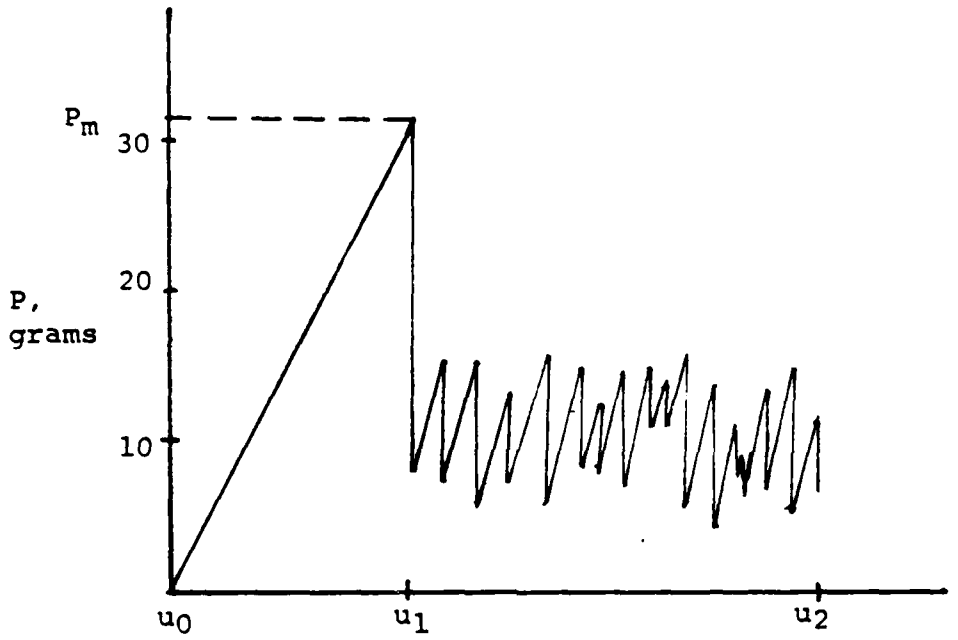
P_m
30
20
P,
grams
10
u_0
u_1
u_2
DISPLACE. OF LOAD APPLICATION POINTS

other authors (9,10).

As mentioned earlier, the single filament pull-out test, like many tests on small volumes of material, exhibites large data scatter. The question to be answered is whether the scatter can be reduced by more careful technique or is inherent in the materials being tested. Our examinations of fiber surface energy show the scatter to be inherent, as discussed later.

III. EXPERIMENTAL

The details for specimen preparation and for carrying out the single filament pull-out test on a universal test machine have been described previously (4). In addition to the many tests done this way, managed to carryout a few tests in the scanning electron microscope with the aid of a tiny tensioning device. For this, the small disc of a matrix surrounding a portion of the single filament 's length was affixed firmly to a mount inside the SEM sample chamber. One of the fiber ends was wound around an externally controlled turning rod. Whie the specimen was observed in the SEM, the rod was turned slowly to place the fiber in tension and produce a debond and pull-out.

The surface energetics of the fiber were investigated using the Wilhelmy wetting force method. As described in detail elsewhere (11), this method monitors the force of interaction between a fiber and a probe liquid as the liquid front advances or recedes slowly along the fiber surface.

IV. RESULTS AND DISCUSSION

A. Direct Observations of Interfacial Cracking

Figure 3 shows the sequence of events during the pull-out process as observed in the SEM. The Figure shows an angle view of a fiber (in this case Kevlar aramid) embedded in a matrix disc. A natural feature

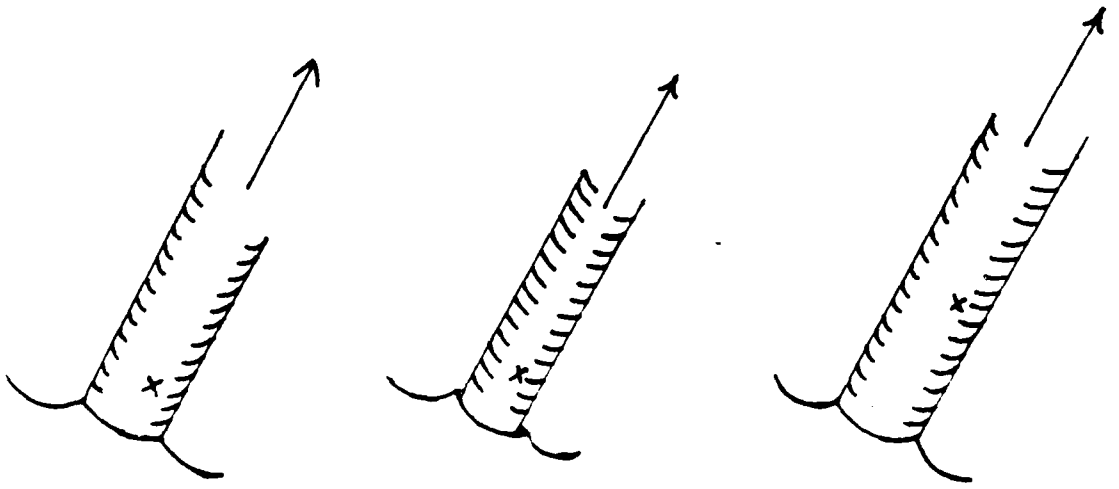

on the fiber (the cross in the drawing) served as a benchmark for judging relative displacement. The left-hand drawing shows the fiber and matrix as the loading is started, before interface cracking starts. With continued application of tensile load, the fiber narrows noticeably and a crack appears at the interface where the fiber enters the matrix (middle). Finally, a sudden upward displacement of the fiber with respect to the matrix occurs, as shown in the drawing on the right. This is a very significant observation since it explains the large instantaneous load drop-off at u_1 in Figure 2. Only a large, sudden extension of the specimen's length, resulting from relative displacement between fiber and matrix, could produce such a load drop-off. It is also important to note that the sudden displacement can occur only after the interface is fully debonded, allowing the matrix to release the fiber. The displacement within the test specimen occurs at a much higher rate than the movement of the test machine grips, producing a relaxation of the load with no time for observable displacement of the grips. The interface debonding can thus be regarded as occuring in the "fixed grip"condition. After debonding and displacement with continued applied load the fiber moves slowly up through the hole in the matrix. The slow steady motion produces the friction seen to the right of u_1 in Figure 2.

B. Fracture Mechanics Interpretation

The actual observed quantities obtained from the single filament specimen and test are the maximum load P_m and the embedded length ℓ. Figure 4 shows a typical plot of P_m versus ℓ for a given fiber - matrix system. Although at small ℓ P_m appears to increase linearly, at larger ℓ it appears to be constant. Attempts at linear correlation over the whole range of ℓ failed, for many such plots of different

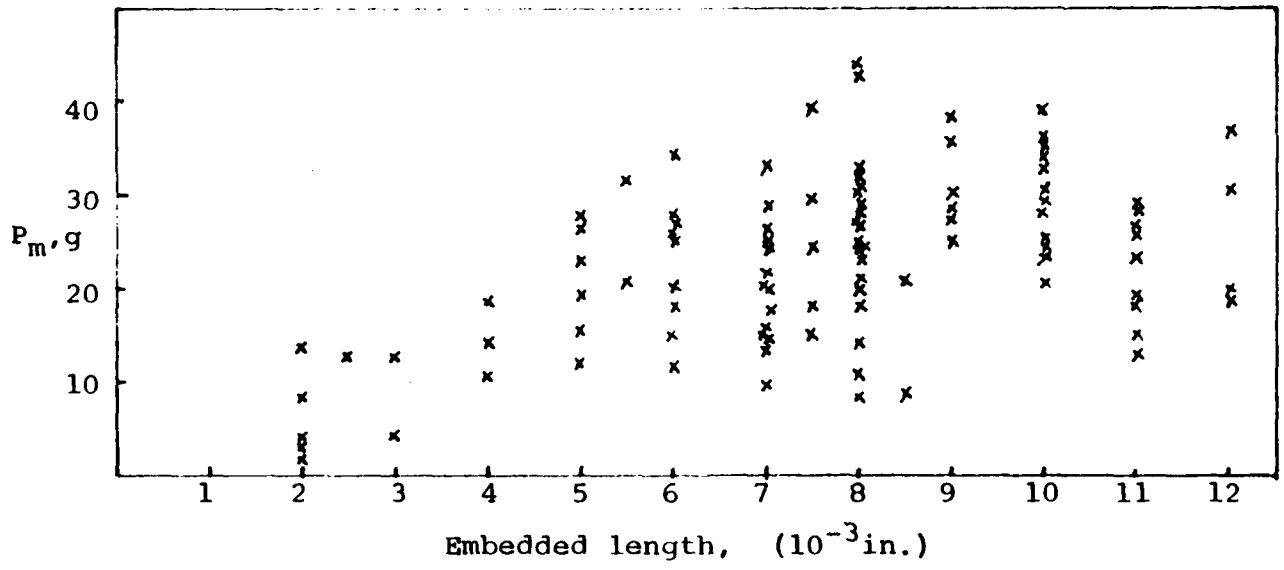
40
30
20
10
P_m, g
1
2
3
4
5
6
7
8
9
10
11
12
Embedded length, (10^{-3}in.)

fibers and matrices. The large scatter in the data makes it difficult to fit the data to a mathematical function with certainty. Furthermore, any function that does fit the data must correspond to an underlying physical meaning.

Because the fracture mechanics approach can mathematically describe the physical failure process, it has the possibility to predict fundamentally correct relations between P_m and ℓ. The P_m vs ℓ curves so derived can then be compared to the experimental data for evaluation of our conception of the physical process. The energy criterion is particularly suitable to describe the failure of the systems in the absence of a clear stress-related criterion.

In the single filament pull-out experiment, the energy required for crack propagation can come from the strain energy stored in the matrix or in the fiber, or in both. The critical specimen load for the crack propagation depends on the fracture surface energy of the two new surfaces formed by cracking, the geometry of the fiber-matrix specimen, and the stiffness of the components of the specimen.

In the discussion immediately below, we will show that if the resin alone supplies the energy, P_m is a rising function of ℓ. We will also show that, by contrast, if the fiber alone supplies the energy, P_m is independent of ℓ. In addition, it will be apparent that at very small ℓ it is mainly the matrix that supplies the energy and at large ℓ the fiber supplies the energy.

In the test configuration shown in Figure 5, an existing crack will extend by length ds if the required amount of energy G_c is supplied. It is assumed that crack initiation readily occurs where the fiber enters the matrix or upon application of the slightest load. Although the single filament pull-out test really experiences fixed

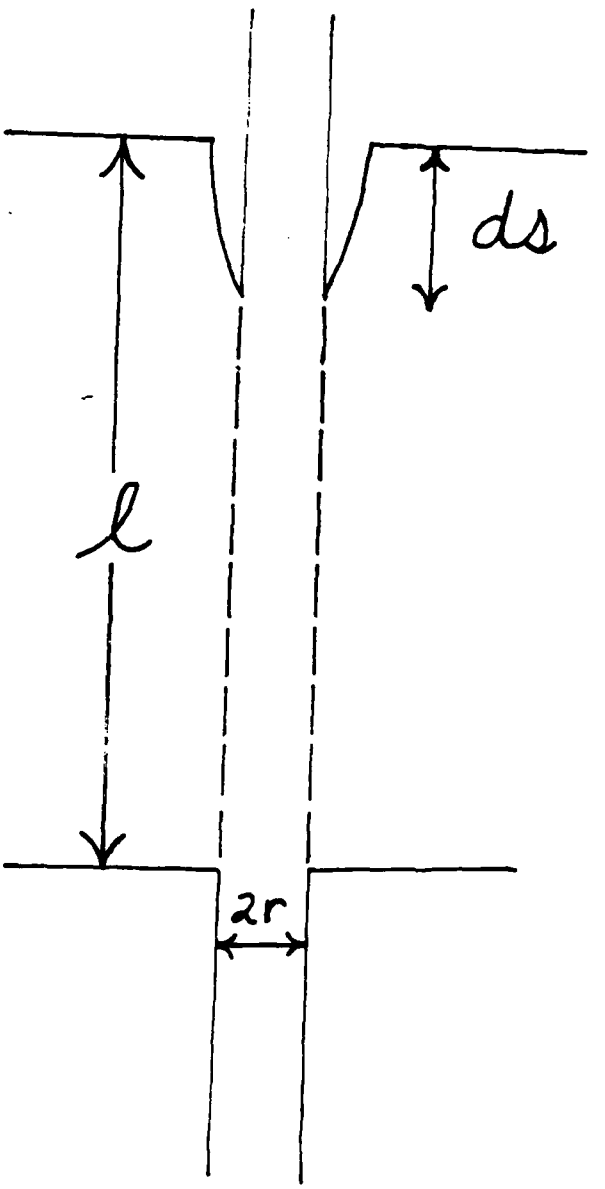
ds
l
2r

grip conditions, the fixed load conditions which give essentially identical results (12) are considered here for the convenience of derivations. Crack propagation will take place when the energy supplied in the constant load condition due to crack extension is equal to or greater than the fracture energy required for cracking. That is,

$$P_m(u_2-u_1)-1/2\ P_m\ (u_2-u_1) = G_c\ 2\ \pi\ rds \qquad (1)$$

where P_m, is the fixed load, u_1 and u_2 are the positions of the load application points before and after crack extension ds, G_c is the strain energy release rate, and r is the fiber radius and ds is the vertical travel of the crack. Thus the left side of the equation is the reduction in potential energy of the system and the right side is the energy consumed by the crack. (G_c times the area of two new surfaces).

Equation (1) can be reduced to:

$$\tfrac{1}{2}\ P_m\ du = G_c 2\pi rds \qquad (2)$$

When the energy for crack propagation comes from the fiber alone, the expression for u is

$$u = \frac{P_m L}{A_f E_f} \qquad (3)$$

where A_f is cross sectional area of the fiber, E_f is the fiber modulus and L is the original free length of the fiber. The derivative of equation (3) gives an expression for du which can be substituted into equation (2).

The result is

$$\tfrac{1}{2}\,\frac{P_m^2\,dL}{A_f E_f} = G_c 2\pi r\,ds \tag{4}$$

Since dL = ds, they can be eliminated, giving

$$\tfrac{1}{2}\,\frac{P_m^2}{A_f E_f} = G_c 2\pi r \tag{5}$$

Rearranging and taking the square root gives the final expression for P_m:

$$P_m = \sqrt{\frac{4\pi r G_c}{\frac{1}{A_f E_f}}} \tag{6}$$

which contains neither ℓ, the embedded length before test, nor L, the free fiber length before test. Therefore, in the case where the energy required to cause crack propagation is supplied by the fiber alone, the pull-out load will be a constant at all ℓ and will depend only on fiber modulus, fiber radius, and interface G_c.

The fiber is likely to supply the energy for crack propagation when the matrix cannot. This would occur if the matrix volume, because of its inherent chemical structure or its overall geometry could not be deformed under load to store much strain energy. However, in many test configurations, the matrix volume as a whole can deform in bending or shear, especially if it is in a thin flat disc shape. Figure 6 shows the configuration and symbols.

In Figure 6, the strain energy (potential energy) builds up in the matrix disc as it deflects under load. The compliance of the matrix disc is defined $C = \delta/P$ where δ is the out-of-plane displacement. The potential energy U_R stored by the matrix is:

$$U_R = \tfrac{1}{2} P\delta = \tfrac{1}{2} P^2 C \qquad (7)$$

We can envision the behavior of C as a function of ℓ. It is reasonable to assume that for a given disc diameter and a given load P placed on the fiber, the larger ℓ values give smaller compliances until at very large ℓ an asymptote is reached where the matrix behaves as an infinite medium. Figure 7 shows this relation. Note that as $\ell \dashrightarrow 0$, $C \dashrightarrow \infty$. For future reference, we have also shown in Figure 7 the derivative of the C vs ℓ curve. Now the strain energy released by a deflected matrix disc as the interface crack propagates by length ds is, at fixed load condition,

$$-dU_R = \tfrac{1}{2} P_m^2 \frac{dc}{ds} \qquad ds = G_c 2\pi r ds \qquad (8)$$

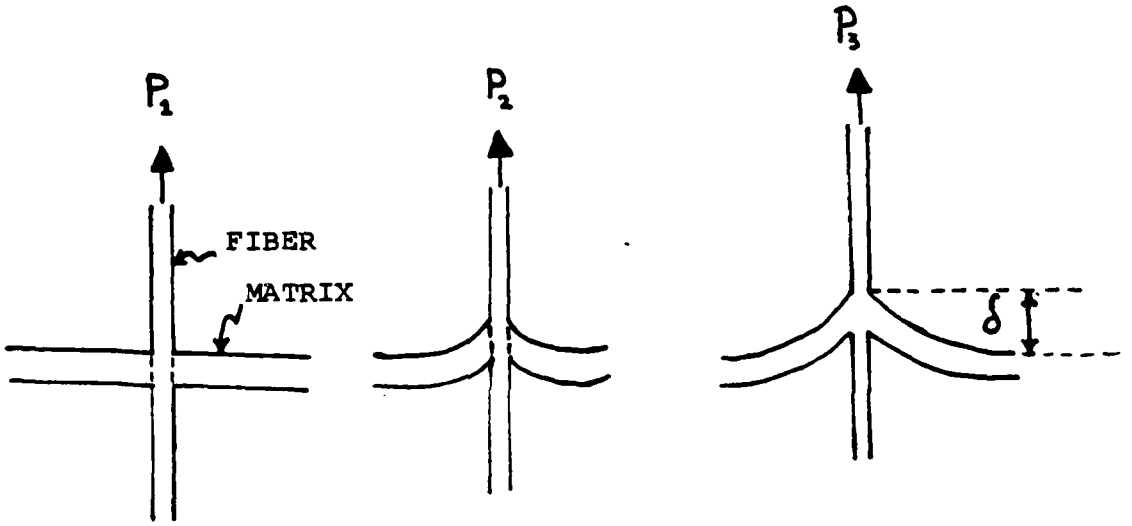

F6

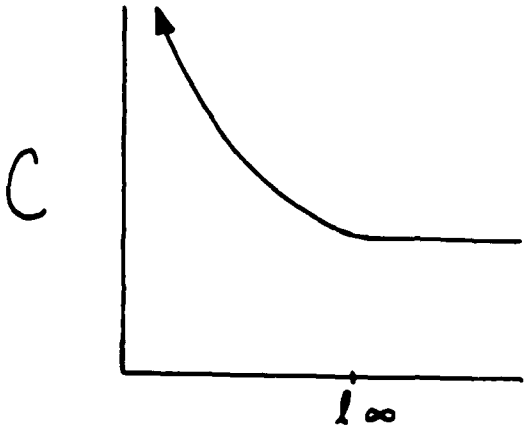

EMBEDDED LENGTH, ℓ

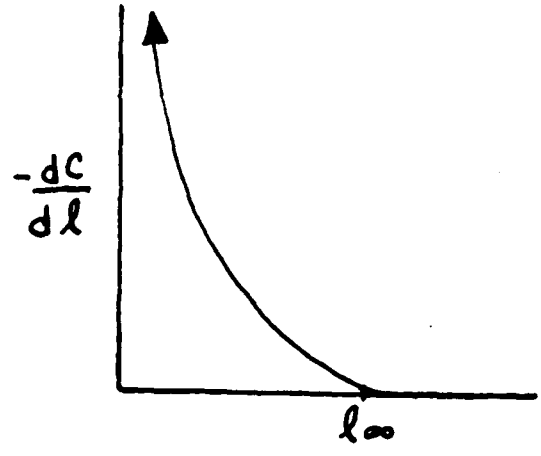

EMBEDDED LENGTH, ℓ

where P now has the subscript m to indicate that it is the maximum P for a single test. Solving for P_m gives:

$$P_m = \sqrt{\frac{4\pi r \quad G_c}{(dC/ds)}} \tag{9}$$

This expression for pull-out force P_m does not contain ℓ explicitly. However, ℓ is contained implicitly in dC/ds. Thus we wish to consider the relation between dC/ds and ℓ . As mentioned previously, the bottom drawing in Figure 7 is a plot of $-dC/d\ell$ versus ℓ and is simply the derivative of the top curve.Where C reaches anasymptote,$dC/d\ell$ reaches zero. As a first order approximation the variation of compliance C within a single specimen as the interface crack length, ds, increases is considered to follow the same shaped curve as a plot of initial compliance C of numerous specimens each of different ℓ. We therefore replace $-dC/d\ell$ in the bottom graph of Figure 7 by $+dC/ds$. The sign difference is due to $d\ell$ and ds decreasing and increasing, respectively. This curve of dC/ds versus ℓ now enables us to know how P_m in equation 9 behaves as a function of ℓ . Figure 8 shows the result, which depicts P_m as a nonlinear increasing function of embedded length before test, ℓ .

In reality, the fiber and matrix contributions must be combined to control the failure process, ie.,

$$\frac{P_m^2}{2E_f A_f} + \frac{P_m^2 \, dc}{2 \, ds} = 2\pi r G_c \tag{10}$$

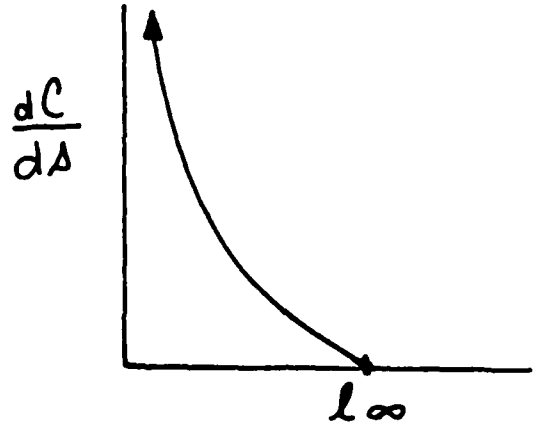

EMBEDDED LENGTH, ℓ

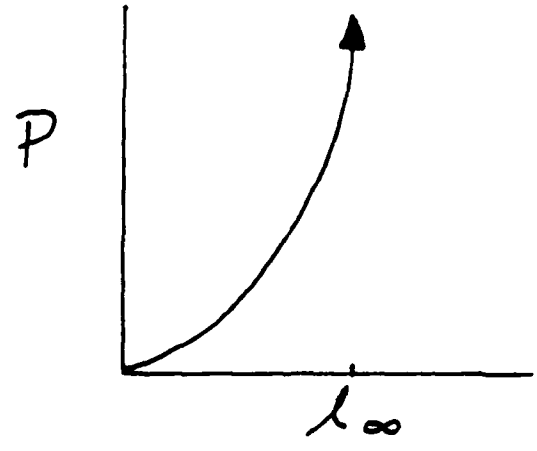

EMBEDDED LENGTH, ℓ

Solving for P_m:

$$P_m = \sqrt{\frac{4\pi r G_c}{\frac{1}{E_f A_f} + \frac{dC}{ds}}} \qquad (11)$$

This relation is depicted graphically in Figure 9, which shows P_m vs ℓ. At low ℓ there will be little or no contribution from the fiber so that the behavior of the specimens is predicted by the curve rising from zero to the horizontal dotted line. At high ℓ, the contribution from the matrix is negligible, allowing the horizontal dotted line to predict the behavior.

Another geometry feature that is predicted to affect the C versus and thus P versus ℓ curves is diameter (2R) of the matrix disc. A larger diameter allows a disc of a given thickness to deflect more readily so that both the C vs ℓ curve and the P_m vs ℓ curve will be shifted to the right as shown in Figure 10. What this means is that even at larger ℓ, if the disc happens to be of large diameter, the pull-out may still be matrix-dominated and the plot of P_m vs ℓ will show an rising P with ℓ. However, for the same range of ℓ values, if the matrix disc is of small diameter, the P_m versus ℓ plot may show fairly constant P, even at small ℓ. This kind of geometry dependence presents problems for those who wish to compare data from different laboratories where slightly different specimen configuration details are used.

The data obtained by Favre and Merienne (2) on carbon fiber embedded in epoxy as well as on aramid fiber embedded in epoxy show

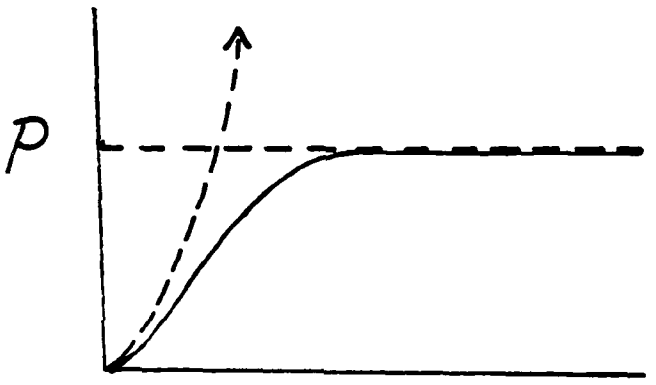
P
EMBEDDED LENGTH, ℓ

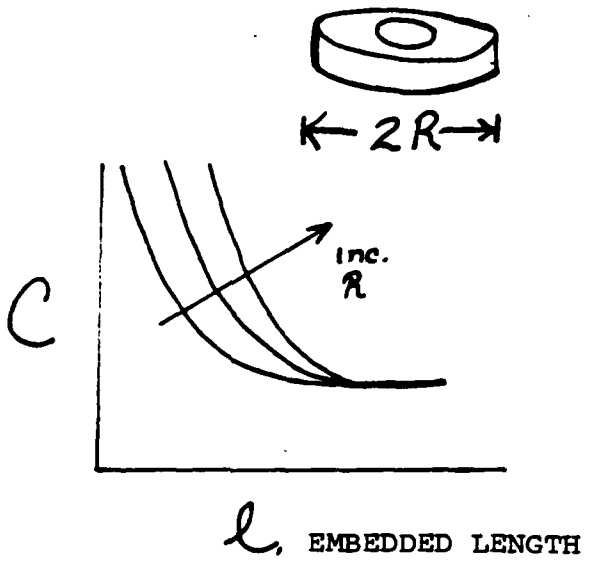
2R
C
inc.
R
ℓ, EMBEDDED LENGTH

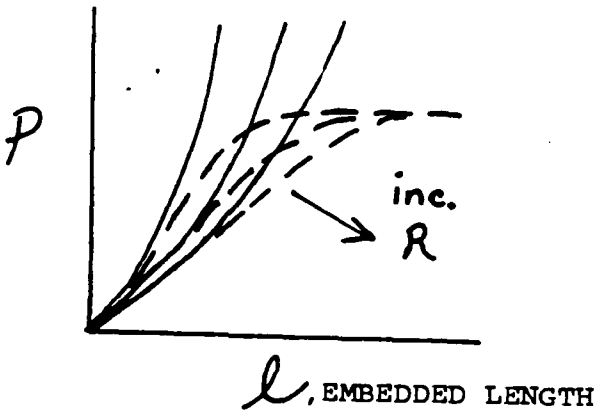
P
inc.
R
ℓ, EMBEDDED LENGTH

the matrix-dominated interfacial fracture. They used a specimen preparation method which resulted in a very thin matrix disc with large diameter. From their published scanning election micrograph, we estimated visually that $2R \approx 100\,\ell$. (Contrary to the practice of these authors in determining the embedded length, we excluded the matrix droplet on the fiber just above the disc in their specimens, since this droplet cannot store and release energy for interfacial crack propagation). Undoubtedly, this wide thin disc would have extensively deformed out-of-plane during the test, thus becoming the source of more than enough energy to drive the crack propagation.

On the other hand, in our laboratory, specimen preparation methods for carbon-epoxy resulted in matrix discs with very small values of $2R/\ell$, ranging from 7 to 15. The reduced compliance of these matrix discs drastically diminished the contribution of the matrix to the energy supplied for fracture. Thus, our data for carbon-epoxy is from fiber-dominated interfacial failure (Figure 11).

The theory is not well enough developed to predict the exact ℓ value at which the change from matrix-dominated to fiber-dominated fracture will occur. While G_c in equation 11 can be computed from the fiber-dominated portion of the curve, (dC/ds) for the matrix-dominated portion cannot be quantitatively determined until experiments are conducted over the whole range of ℓ. The intersection of the matrix-dominated curve with the fiber-dominated curve is determined not only by specimen geometry, but also by the other quantities implicit and explicit in equations 9 and 11 : fiber modulus and radius and matrix shear and bending modulus.

The single filament pull-out test results comparing Kevlar 49 to Kevlar 29 were consistent also with the model we have presented here.

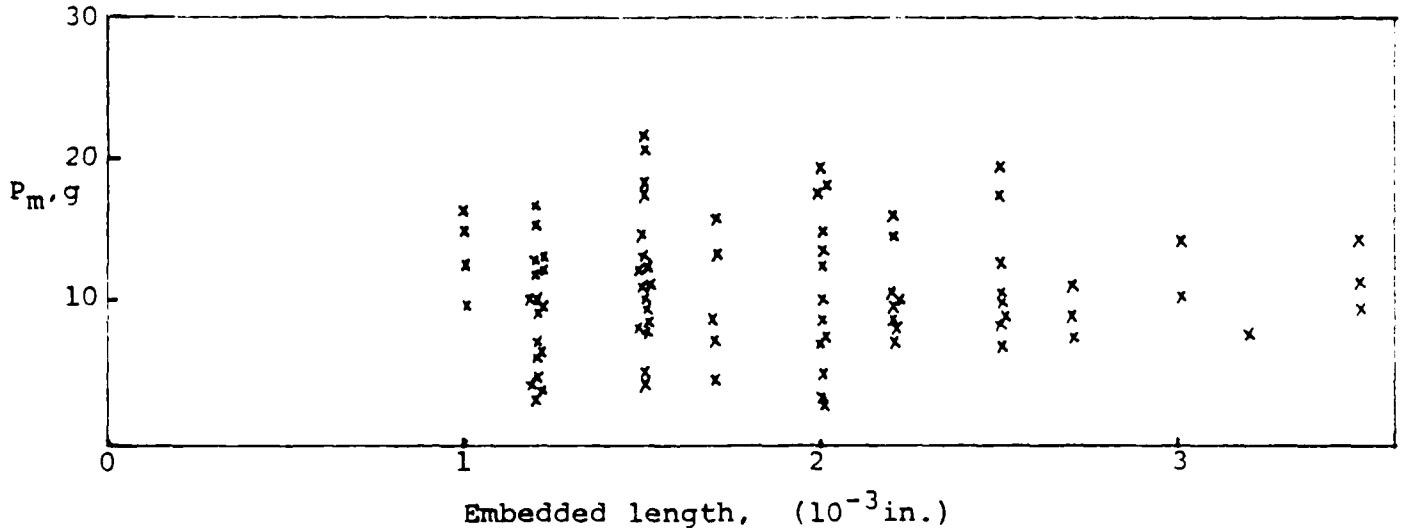

F 11

Both aramid fibers have identical surface energy (13) and nearly equal radii. For the comparison the same matrix and cure cycle were used to ensure equal G_c values for both systems. Data were collected over a wide range of ℓ and P_m versus ℓ curves were plotted and examined. According to equation 11 , since the modulus of Kevlar 49 is twice that of Kevlar 29, the pull-out load for the fiber-dominated pull-out process should be higher by a factor of $\sqrt{2}$ for Kevlar 49. Considering only the higher ℓ values, where P_m is observed to be constant, we found that P_m for Kevlar 49 was 32.1 ± 7.69MPa and P_m for Kevlar 29 was 24.9 ± 7.42MPa. As expected, the average for Kevlar 49 is higher by approximately $\sqrt{2}$.

C. Study of the Source of Scatter

While the energy balance model presented above is only qualitative, the discussion below of scatter in the experimental data focusses on quantitative aspects. Those who carry out the single filament pull-out test report large scatter in the data. This has been a cause of concern because one assumes that small misalignments and maladjustments could greatly affect the results in this "microtest". However, another source of scatter is the inherent inhomogeneity of small volumes of material being tested. The volumes of the materials used in a typical pull-out test may be too small for homogeneities to be averaged. Furthermore, if the pull-out process is crack propagation rather than simultaneous yield of the whole bonded interface, the failure load depends upon the even smaller volume of material near the top of the original embedded length.

Wetting force studies on the surface energetics of engineering fibers offer insight into the material inhomogeneity. It is well known by surface chemists that the surfaces of solids, even when

mechanically perfectly smooth, are chemically heterogeneous. This chemical heterogeneity is what produces the ubiguitous contact angle hysteresis (14,15). Wetting force measurements carried out on small diameter fibers provide a good measure of the scale of the surface chemical heterogeneity. Figure 12 shows the advancing and receding wetting force values as water, a liquid highly sensitive to changes in surface polarity, moves up (advances) and down (recedes) a short length of Kevlar fiber. The variations in amplitude of wetting force along the fiber length arise from variations in the fiber surface's interaction with the water line. This in turn originates from the fiber surface chemical heterogeneity. By converting the wetting force values at any point along the fiber to contact angle values the corresponding work of adhesion, W_A at that point may be computed:

$$W_A = \gamma_L (1 + \cos\theta) \qquad (12)$$

where γ_L is surface tension of the contacting liquid and θ is the advancing or receding contact angle. We see that within a 4.0 mm length of fiber in the advancing mode a low W_A of 93 ergs/cm^2 was obtained and a high of 127 ergs/cm^2, values which differ by 12 and 20% respectively, from the average of 106 ergs/cm^2. Even within as short a length as 0.1mm, the variation can be large. Because these variations are reproducible on repeated runs we know they are not from vibrations or electrical noise. Figure 13 shows the wetting force trace as ethylene glycol, a liquid less sensitive than water to polar regions on the fiber surface, advances and recedes along the fiber length. This trace also shows large variation in W_A from spot to spot along the fiber length. In the advancing mode, the high and low values of 70.7 and 90.4 ergs/cm^2 differ by 14 and 10% respectively from the

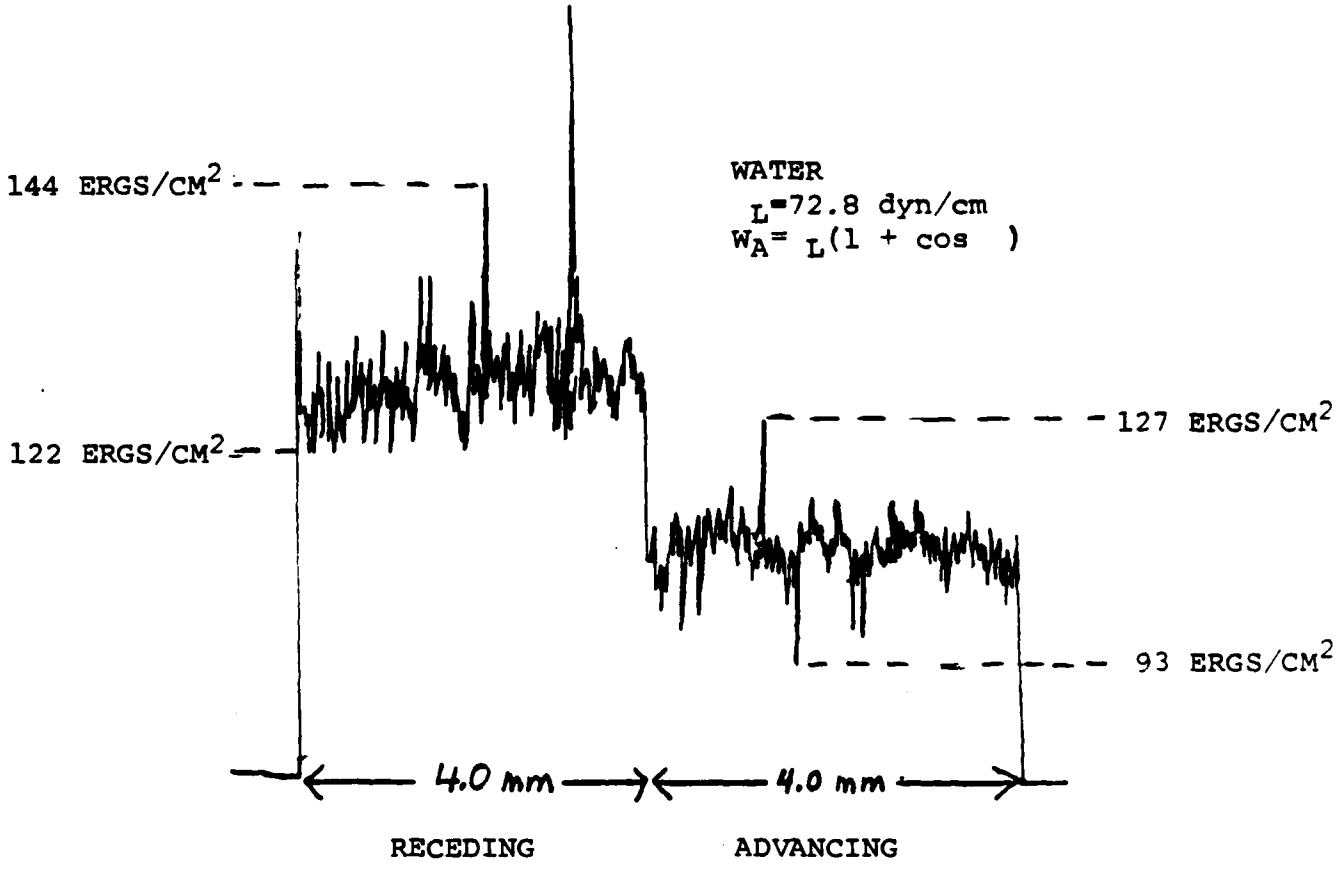
144 ERGS/CM2
WATER
L=72.8 dyn/cm
WA= L(1 + cos)
122 ERGS/CM2
127 ERGS/CM2
93 ERGS/CM2
4.0 mm
4.0 mm
RECEDING
ADVANCING

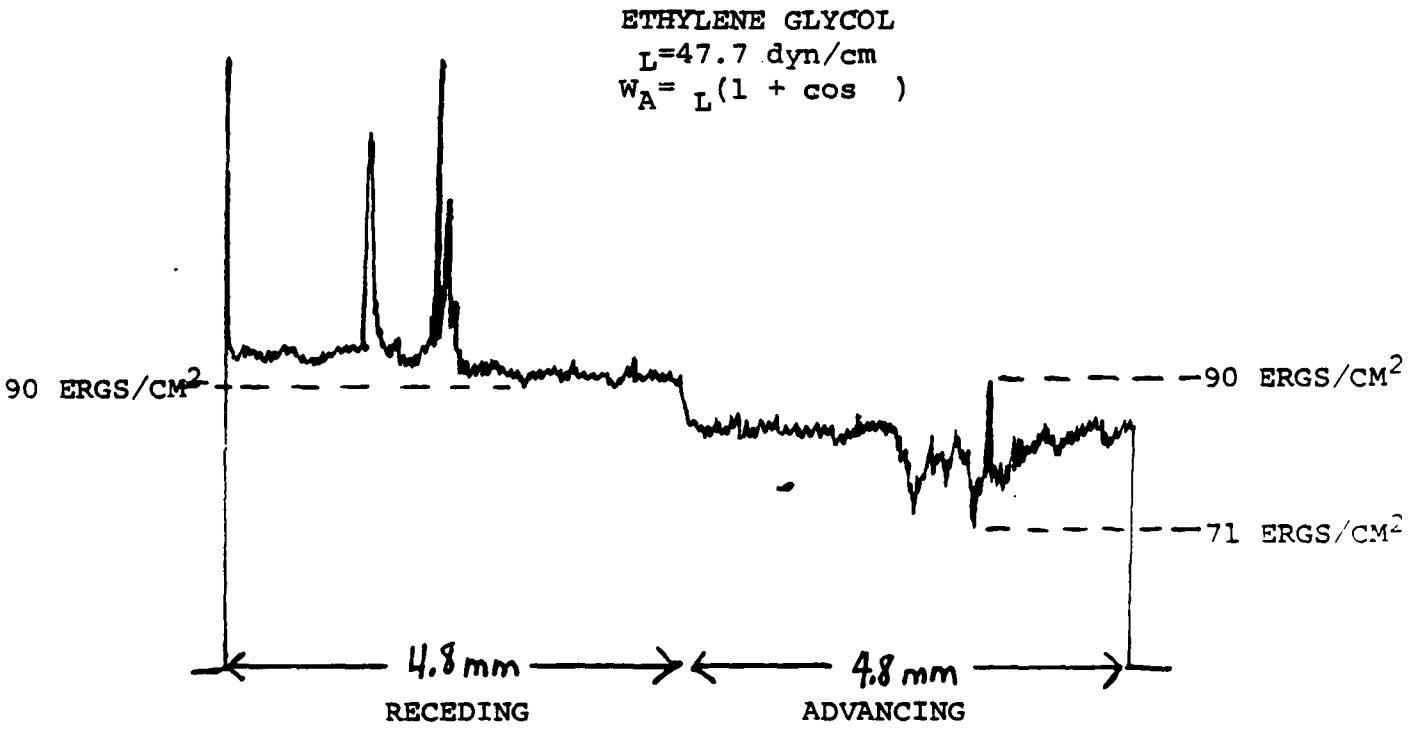
ETHYLENE GLYCOL
L=47.7 dyn/cm
$W_A = {}_L(1 + \cos\ )$
90 ERGS/CM^2
90 ERGS/CM^2
71 ERGS/CM^2
4.8 mm
4.8 mm
RECEDING
ADVANCING

F13

average of 82.3 ergs/cm^2.

The interaction between Kevlar and Typical liquid epoxy resins, the latter too viscous for accurate wetting force studies, are bracketed by the Kevlar-water and the Kevlar-ethylene glycol systems just discussed. Therefore a good estimate of the Kevlar-epoxy interaction is an average of 90 ergs/cm^2 with a variation of $\pm$15%.

It is reasonable to assume that the interfacial interaction between a fiber and solid matrix would echo the fiber-liquid interactions and also display large local variations. Thus we would expect large variation in the pull-out load in mechanical tests of the interface strength when crack propagation is the failure mechanism. Therefore, we conclude that most of the scatter in the pull-out load values is inherent in the interface itself and cannot be reduced.

There is another type of single filament test that has been used to indirectly measure interfacial adhesive strength. This is the single filament fully embedded in a dogbone of cast resin. An average interfacial strength is computed from measuring the many broken lengths of the single filament after tensile loading. There is a large (>20%) scatter in these broken lengths (16). However, the average value of the broken lengths in one dogbone differ little (<10%) from that of another. Here, one dogbone is like a batch of many specimens. Similarly, comparison of average values of P_m for different batches of single filament pull-out tests shows good agreement between batches. The agreement between averages shows that local variation in the interface is reproducible, which in turn demonstrates that it is inherent and not an artifact.

CONCLUSIONS

The single filament pull-out test is an attractive test for many researchers because it gives a direct measure of the fiber-matrix bond strength of a composite material. However, the following conclusions indicate that it must be used with caution.

a) When the matrix disc has compliance and can store energy as it can for low ℓ (or high $2R/\ell$), the failure may be matrix-controlled and P_m will be a rising function of ℓ.

b) When the matrix disc has negligible compliance compared to the fiber, the failure is fiber-controlled and P_m is independent of ℓ.

c) Because crack propagation rather than simultaneous debonding is often the failure mechanism, failure load is dependent on an extremely small interface area at the crack tip.

d) Engineering fibers have large local variations in surface energy, leading to large local variations in fiber-matrix adhesion.

These conclusions lead to the following recommendations:

a) Only data from exactly the same test configurations should be compared.

b) The computation P/A can be misleading and should not be used over the whole range of ℓ. It may be used in the region where failure is matrix-dominated and P_m vs ℓ approximates a linear relation; or it may be used for P_m values at a single selected ℓ.

c) For comparing different populations, P_m values should be obtained over a wide range of ℓ, so that the matrix-dominated and fiber-dominated failure regions can be clearly seen. Each region can then be compared.

REFERENCES

1. G.D. Andreevska and Yu. A. Gorbatkina, Ind. Eng. Chem., Prod. Res. Develop., 11, 24 (1972).

2. J.-P. Favre and M.-C. Merienne, Int. J. Adhesion and Adhesives, 1, 311 (1981).

3. D.B. Eagles, B.F. Blumentritt, and S.L. Cooper, J. Appl. Polym. Sci., 20, 435 (1976).

4. L.S. Penn and S.M. Lee, Fibre Sci. and Technol., 17, 91 (1982).

5. P.S. Chua and M.R. Piggott, Comp. Sci. and Technol., 22, 33 (1985).

6. L.B. Greszczuk, in "Interfaces in Composites," ASTM STP 452, American Society for Testing and Materials, Philadelphia, Pennsylvania 1969, p. 42.

7. P. Lawrence, J. Mat. Sci., 7, 1 (1972).

8. R.J. Gray, J. Mat. Sci., 19, 861 (1984).

9. M.R. Piggott, A. Sanadi, P.S. Chua, and D. Andison, International Conference on the Composites Interface, Cleveland, Ohio, May 27-30, 1986.

10. P.S. Chua and M.R.Piggott, Compos. Sci. Technol. 22, 107 (1985).

11. B. Miller, L. Penn, and S. Hedvat, Colloids and Surfaces. 6, 49 (1983).

12. D. Broek, "Elementary Engineering Fracture Mechanics", Martinus Nijhoff, The Hague, 1982, p. 115.

13. L. S. Penn, F. A. Bystry, and H.J. Marchionni, Polymer Composites, 4, 26 (1983).

14. R.E. Johnson and R.H. Dettre, J. Phys. Chem., 68, 1744 (1964).

15. A.W. Neumann and R.J. Good, J. Colloid and Interface Science, 38 341 (1972).

16. L. Drzal, Michigan State University, East Lansing, Michigan personal communication.

ACKNOWLEDGEMENTS

This research was supported in part by the office of Naval Research. The authors also gratefully acknowledge the contribution of Ms. Michelle Shelton of Midwest Research Institute, Kansas City, Missouri, and of Mrs. Han Xin Zhou of China Textile University, Shanghai, and Dr. Dennis Artman and Mr. Irv Nusynowitz of Ciba-Geigy, Ardsley, New York.

FIGURE CAPTIONS

FIGURE 1 Various geometries that can be used for the single filament pull-out test. Tension is applied to the fiber to pull it from the matrix disc. The embedded length at the beginning of the test is designated ℓ.

FIGURE 2 Typical force versus displacement trace for an individual pull-out test. The displacement recorded is that of the test machine grips. The filament is placed in tension starting at u_o; the debonding is completed and the filament first slips with respect to the resin at u_1; the filament's free tail pulls up through the resin disc from u_1 to u_2, showing frictional force.

FIGURE 3 Sequence of events in a single filament pull-out test as viewed in the scanning electron microscope. At left, part of the filament's length has been embedded in a disc-like block of matrix, and tension is applied to the fiber. At center, continued tension causes a crack to develop in the fiber-matrix interface at the top of the embedded length. At right, the crack has just finished propagating the full length of the interface, and the fiber, released from the resin, has made a sudden large displacement upward. After this, under further tension, the filament continues to pullup through the matrix.

FIGURE 4 Typical plot of P_m versus ℓ for an engineering fiber (Kevlar 29) embedded in epoxy matrix (diglycidyl ether of bisphenol A cured with triethylene tetramine), At very small ℓ's, the P_m values are low. They rise with increasing ℓ and appear to reach an asymptote. Large scatter is due to inherent variation in interfacial adhesion. cured at 120°C for 3 hours.

FIGURE 5 Diagram of single filament with part of its length embedded in cured matrix. The embedded length before debonding is ℓ. Interface cracking will occur if potential energy released by strained test specimen as a result of interface crack extension by length ds is equal or greater than required to form the two new crack surfaces ($-dU_R = G_c\, 2\pi r ds$).

FIGURE 6 Diagram of matrix disc deflecting as fiber is loaded in tension. Compliance ($C = \delta/P$) of disc determines how much energy can be stored by matrix at a given load P.

FIGURE 7 At a given load, P, the larger the disc thickness (or embedded length) ℓ, the lower the disc compliance, as shown in the graph at top. Finally, at some ℓ, the disc is equivalent to an infinitely thick disc and C reaches a lower limit (asymptote). The rate of change in disc compliance as a function of ℓ is shown in the graph at bottom.

FIGURE 8 Graph of change in compliance per unit interface crack length as a function of original embedded length (top). This graph is derived by analogy from the graph of $dC/d\ell$ versus ℓ on the basis that $dC/d\ell = dC/ds$ for small crack length. The bottom graph of P_m versus ℓ is derived from the top graph through the equation $P = \sqrt{4\pi r G_c/(dC/ds)}$

FIGURE 9 Superimposed graphs of P_m versus ℓ for matrix controlled interfacial failure and for fiber controlled interfacial failure. If ℓ is low enough then control of failur process will be usurped by matrix and no data points will appear in region of horizontal dotted line. Similarly, when ℓ is high enough that process is fiber-controlled, no data will appear in region of rising dotted line.

FIGURE 10 Graphical representation of the effect of increasing the matrix disc diameter. The curve of matrix compliance versus ℓ will shift to the right (top). Consequently, the curve of P_m versus ℓ will also shift to the right.

FIGURE 11 Plot of P_m versus ℓ for carbon fiber-epoxy (AS4 fiber in diglycidyl ether of bisphenol A cured with triethylene tetramine, at 70°C for 65 h). Failure process is fiber-controlled over most of the range of ℓ values due to small diameter to thickness ratio of matrix disc and lack of disc compliance.

FIGURE 12 Wetting force trace made by water advancing and receding along the length of a Kevlar fiber. The variation in wetting force (vertical axis) is due to chemical heterogeneity inherent in the smooth surface of the fiber. Computed work of adhesion values are indicated for selected wetting force values.

FIGURE 13 Wetting force trace made by ethylene glycol advancing and receding along the length of a Kevlar fiber. The variation in wetting force (vertical axis) is due to chemical heterogeneity inherent in the smooth surface of the fiber. Computed work of adhesion values are indicated for selected wetting force values.

END

3-87

DTIC